Indian Journal of Pure & Applied Physics
Vol. 62, September 2024, pp. 759-763
DOI: 10.56042/ijpap.v62i9.11572

Exploring the Impact of CeO_2 Doping on the Structure and Magnetism of Hematite Nanoparticles

Seema[a*], Meenakshi[b], Rajesh Sharma[c*] & Seema[d]

[a]Department of Physics, Research Scholar, Baba Mastnath University, Rohtak 124 021, India
[b]Department of Physics, Faculty of Sciences, Baba Mastnath University, Rohtak 124 021, India
[c]Department of Physics, Faculty of Sciences, M.N.S Govt. College, Bhiwani 127 021, India
[d]Department of Physics, Faculty of Sciences, Pt. N.R.S Govt. College, Rohtak 124 001, India

Received 2 June 2024; accepted 1 August 2024

In this study, Fe_2O_3 nanoparticles were doped with varying concentrations of cerium oxide (CeO_2) (5%, 10%, and 20%) were synthesized by using a microwave treated co-precipitation method and thereafter, calcined at 600°C temperature for 2hrs. The X-ray diffraction (XRD) analysis revealed that all calcined samples exhibited hexagonal crystalline structures, with a decrease in grain size from 60.547nm to 47.060 nm with increasing CeO_2 concentration. Fourier transform infrared (FTIR) spectroscopy confirmed characteristic peaks of hydroxyl group at 3541 cm^{-1} and 1624 cm^{-1}, while sharp peaks of 471 cm^{-1} were identified as the O-Ce-O stretching vibrational band. The observed FTIR patterns were consistent with the XRD results supporting the influence of differing ionic radii between Ce^{4+} and Fe^{3+} ions. The Magnetic properties were examined through by using a vibrating sample magnetometer (VSM) and revealed that saturation magnetization peaked at 5% CeO_2 dopant concentration (M_s = 33.2×10^{-2} emu/g), while coercivity reached its maximum at 10% concentration (H_c = 548.26 O_e). Conversely, remnant magnetization (M_r) decreased (4.3×10^{-2}, 3.1×10^{-2}, and 0.9×10^{-2} emu/g) with increasing cerium oxide concentration (5%, 10%, and 20%).

Keywords: Ceria-doped Fe_2O_3 nanoparticles; XRD; FTIR; Structural and Magnetic properties

1 Introduction

Nanomaterials have attained lot of attention in recent years due to their versatility across various biomedical applications, from diagnostics to therapeutics. Metal-oxide-based magnetic nanoparticles have been extensively researched for their use as contrasting agents in magnetic resonance imaging (MRI)[1–3] and in the treatment of hyperthermia[4-7].

Additionally, iron oxides are well known and important due to their stability, eco friendly, cost-effectiveness and finding applications in adsorbents, catalysis, and data storage. Iron oxides, semiconductors with band gaps between 1.9 eV. and 2.2 eV, exhibit four distinct crystal phases: α-Fe_2O_3 (rhombohedral), β-Fe_2O_3 (cubic), γ-Fe_2O_3 (cubic), and ε-Fe_2O_3 (orthorhombic). Hematite, known as α-Fe_2O_3, is the highest stable iron oxide with unique chemical thermo dynamical, electrical and magnetic properties[8–14]. Its non-toxic nature and corrosion-resistant makes it an attractive material for various industries.

The Cerium(Ce) is a rare earth metal and the initial position in the lanthanide series of the periodic Table 1, exhibits intriguing properties attributed to the shielding effect of its 5p and 4d electrons on the 4f orbitals. The Cerium element can adopt both 3^+ and 4^+ oxidation states, resulting in the formation of cerium oxide, represented as CeO_2 and Ce_2O_3. But at the nanoscale, as nanoparticles diameter decreases, an increase in the number of 3^+ sites on the surface, and oxygen atoms are lost[15,16]. Cerium oxide nanostructures find applications in energy conversion, cosmetics, storage, mechanical polishing, catalysis, solar cells, gas sensing, biomedical applications, and automotive exhaust treatments[17].

Although various synthesis methods, including hydrothermal, sol-gel, sonochemical, combustion, thermal decomposition, polyol, and co-precipitation

Table 1 — illustrates the computed X-ray diffraction (XRD) spectrum of CeO_2-doped Fe_2O_3 nanoparticles calcined at 600 °C for two hours.

Nanoparticles concentration	Most intense peaks position	(FWHM) (beta)	Grain size(D)	Strain in (ε)	Dislocation density
5%	33.202	0.143	60.547	0.0365	0.272
10%	33.220	0.164	52.790	0.0418	0.358
20%	33.243	0.184	47.060	0.0469	0.451

*Corresponding author: (E-mail: seemabisla07@gmail.com)

were employed to fabricate CeO_2-doped Fe_2O_3 nanoparticles. Among these, the co-precipitation method is used due to its unique benefits, including uniform doping element distribution, low cost, high purity, reduced energy-consumption, with minimum environmental impact, is suitable for large-scale production and it also requires minimum preparation time. But traditional methods are known for their lengthy processes, use toxic compounds, and the need for expensive equipment, which can hurt human health and the environment.

The present work explore the synthesis of ceria (5%, 10% and 20%) doped Iron oxide nanoparticles via microwave irradiated chemical co-precipitation method, thereafter, as synthesized samples were calcined at temperature 600 ^oC for 2 hours constant heating. The structural studied of all the samples proved that newly doped sample were hexagonal structure corresponds to well known hematite formation of Fe_2O_3. However, the presence of Ce^{4+} ion were seen in XRD pattern with additional peak position 2θ28.4^o and were analogous to JCPDS-PDF 04-018-4988. The magnetic properties of material were examine by Vibrating sample Magnetometers tools and VSM results residual magnetization repeatedly decreases with increases of dopant concentration and nature of newly synthesized material were super paramagnetic behaviour. So, therefore, the resulted material may be used for enhanced applications such as electromagnet etc.

2 Experimental details

2.1 Synthesis

All the chemicals used in this study were Analytical in grade and not be purify at laboratory scale. The Iron chloride ($FeCl_3.6H_2O$) and Cerium nitrate ($Ce(NO_3)_39H_2O$) were mixed in 100ml of doubly ionized water at the proper mass concentration. However, the resulting solution was frequently and gently mixed with a magnetic stirrer for an hour at room temperature and received a mustard colour. Subsequently, ammonia was added to the obtained solution to get it to the desired range of 8.5 pH, which was measured with an electrode pH meter. The precipitate was passed through HOFFMAN filter paper to start the filtration process. After that precipitate was cleaned distilled water and ethanol to remove impurities, and the filtered cake was dried in the microwave for 15 minutes at 150 °C on two settings. Then, it was calcinated at 600 °C for 2 hours. Subsequently, the fine powder samples were obtained after being crushed in an agate mortar respectively stored in an insulated containers. The calcined samples at 600 ^oC/2hrs samples were sent to the SAIF, Punjab University, Chandigarh and CEERI Pilani for as-desired characterization results.

3 Characterisation

A "Bruker X-ray diffractometer" at wavelength (1.5406nm) the Central Instrumentation Facility (CIF), Lovely Professional University (LPU), Phagwara (Punjab), was used to analyse the sample for an X-ray analysis. The scanning range of the device was 10^o and 80^o. The "Perkin Elmer Spectrum RX-IFTIR" was employed at the Sophisticated Analytical Instrumentation Facility (SAIF) in Punjab to examine the infrared characteristics of the materials in the 400–4000 cm^{-1} wave number range. The magnetic properties of samples were examined at lab of Central Electronics Engineering Research Institute (CEERI), Pilani a segment of the Council of Scientific and Industrial Research (CSIR) New Delhi.

4 Results and discussion

4.1 Structural Properties

The diffraction patterns of both undoped and CeO_2 doped Fe_2O_3 nanoparticles with concentration (5%, 10% and 20%) and calcined at 600 °C/2hrs is shown in Fig. 1.

The results of X-ray diffraction demonstrate that Fe_2O_3 exhibits a hexagonal structure (JCPDS card # 89-0596)[18]. Diffraction peaks related to CeO_2 were detected 28.82^o, 47.70^o, 56.65^o and 69.84^o indicating that Fe_2O_3 crystal lattice has been corporated with CeO_2 ions (Appendix-2, reference number:

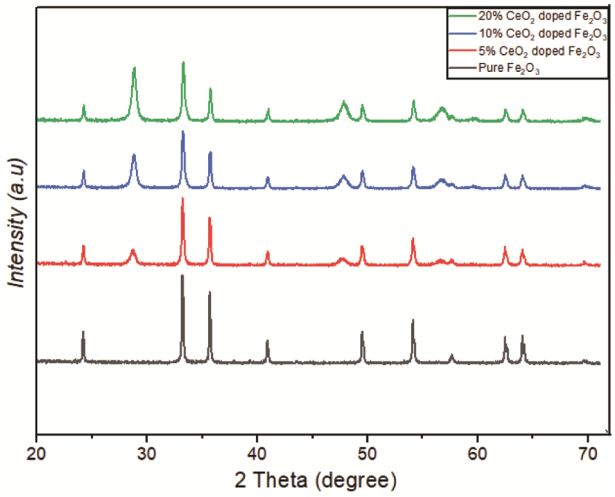

Fig.1 — illustrates the X-ray diffraction of the material as quoted in figure and calcined at 600 °C for two hours

PDF 04-018-4988)[19]. The most intense peak of undoped at 33.177° and CeO_2 doped Fe_2O_3 (104) positions at 33.202°, 33.220°, and 33.243° were used to determine the grain size using scherer Eq. 1.

$$D=K\,\lambda/\beta\cos\theta \quad \ldots(1)$$

The parameters D, K (0.98), λ, β, and θ represent the crystallite size, form factor, wavelength of the source, FWHM(Full width half maxima) and diffraction angle[20]. The grain sizes were found 60.547nm, 52.79nm and 47.06nm respectively, with increasing concentration of CeO_2, the grain size decreased. From XRD graph it was appear that small shifting of most intense peak occur toward smaller 2θ position and it might be due to uniform strain occurred in Fe_2O_3 lattice with presence of Ce^{4+} ions. However, the broading of peak were recorded with increase dopant concentration ceria and may be caused by vacant f-orbital e^- in Ce atom[21]. Fig. 1 shows that theFe_2O_3 lattice's grain size decreases due to the presence of Ce^{4+} atoms.

The prepared materials micro-strain is explained by Eq. 2

$$\text{Strain } (\varepsilon) = \beta\cos\theta/4 \quad \ldots(2)$$

When determining the crystalline size, the (104) plane is recommended. According to the information in the Table 2, indicates that an increase in strain accompanies an improvement in sample quality. It means that the material is changing at the atomic level, which leads to a higher number of lattice defects. This can have significant implications on the material's strength, power and appearance.

The dislocation density of the crystal structure for preferred (hkl) orientation values is calculated to using Eq. 3[22].

$$\text{Dislocation density } (\delta) = 1 / D \quad \ldots(3)$$

Dislocation density shows that the number of lattice imperfections increases as the crystallite size decreases.

The tabular data shows that grain size decreases with increase of ceria concentrations and it might be due to uniform strain increases with ceria dopant concentrations.

Table 2 — illustrates the computed Vibrating sample magnetometers of CeO_2-doped Fe_2O_3nanoparticles calcined at 600 °C for a duration of two hours.

600°C for 2 hours	M_s(emu/g)	M_r(emu/g)	H_c (O_e)	(M_r/M_s)
5%	33.2×10^{-2}	4.3×10^{-2}	529.56	0.129
10%	25.2×10^{-2}	3.1×10^{-2}	548.26	0.123
20%	20.2×10^{-2}	0.9×10^{-2}	234.19	0.044

4.2 FTIR Spectroscopy Study

The valuable information is categorized using the FTIR approach to the chemical composition, molecular structure, and functional groups found in the samples of CeO_2-doped iron oxide nanoparticles[23].

Figure 2 presents the FTIR spectra of CeO_2-doped Fe_2O_3 samples with varying doping concentrations (0%, 5%, 10%, and 20%) across the wave number range of 400 cm^{-1} to 4000 cm^{-1}. The peaks identified at 3541 cm^{-1} correspond to the O-H bending mode of hydroxyl groups, whereas the bands observed at 1624 cm^{-1} represent the asymmetric and symmetric vibrations of -CH_3 groups[24,25]. The 1370 cm^{-1} peak indicates the presence of NO_2 and CO_2 in the sample. The sharp peaks observed at position 471cm^{-1} and 614 cm^{-1}were attributed by O-Fe-O molecule and O-Ce-O molecule stretching vibration respectively[26-28]. The FTIR results support the XRD results and conformed that pure Fe_2O_3 and ceria doped Fe_2O_3 nanocrystilline were formed in present work.

4.3 Magnetic Properties

In this study, the magnetic behavior of CeO_2-doped Fe_2O_3 nanoparticles was investigated after annealing

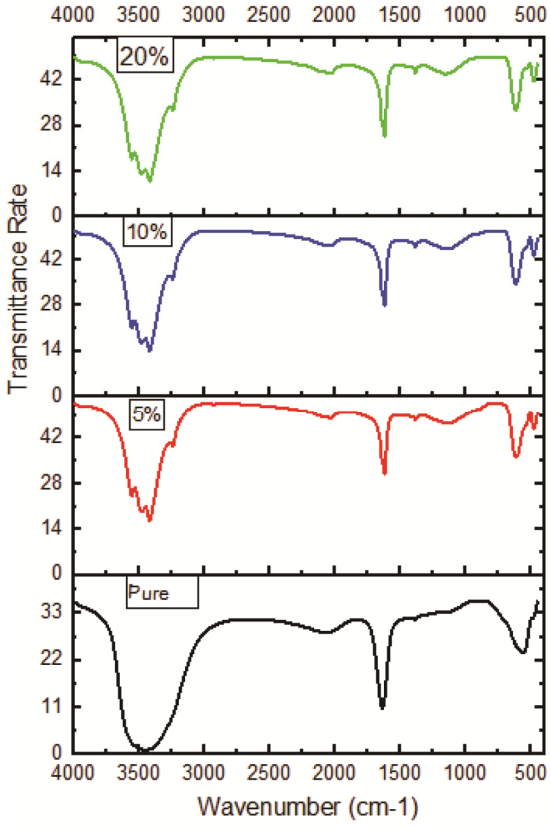

Fig. 2 — illustrates the infrared spectrum of the material as quoted in figure and calcined at 600 °C for two hours

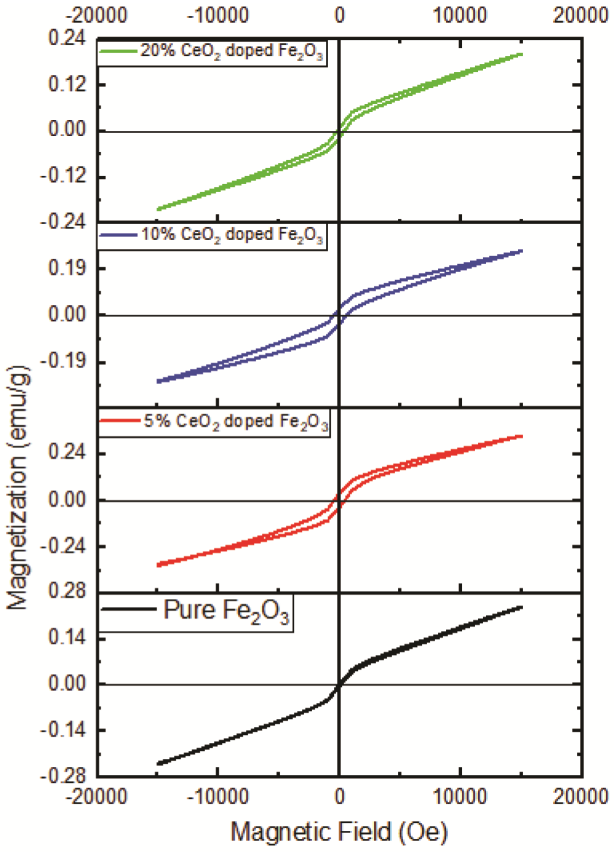

Fig. 3 — illustrates the vibrating sample magnetometers of the material quoted in figure and calcined at 600 °C for two hours

at 600 °C and exposure to varying magnetic fields using a VSM at room temperature (300 K). The magnetic field strengths ranged from -20 kOe to +20 kOe.

The Vibrating sample magnetometer characterization results of Ceria (5%, 10% & 20%) doped Fe2O3 samples calcined at 600 °C/2hrs , depicted in Fig. 3, reveal the remnant magnetization (M_r), saturation magnetization (M_s), and coercivity (H_c) values of CeO_2-doped iron oxide nanoparticles. The saturation magnetization values were found to be 33.2 × 10^{-2} emu/g, 25.2 × 10^{-2} emu/g, and 20.2 × 10^{-2} emu/g for the respective doping concentrations. The corresponding remnant magnetization values were measured as 4.3 × 10^{-2} emu/g, 3.1 × 10^{-2} emu/g, and 0.9 × 10^{-2} emu/g. Additionally, the coercivity values were observed as 529.56 O_e, 548.26 O_e, and 234.19 O_e, respectively. These results indicate a trend of decreasing M_s and M_r values with increasing CeO_2 doping concentration, while the coercivity values exhibit variations across the different doping levels. Overall, these findings show that CeO_2-doped iron oxide nanoparticles have magnetic properties that depend on the amount of doping.

Smaller particle sizes exhibiting decreased M_s values due to spin disorder at the nanoparticles' surface. The past study revealed that the size of dopant ions is smaller than that of host ions and altered the magnetic behavior of the material *i.e*. CeO_2 in bulk have diamagnetic in nature and ceria doped iron oxide at nanoscale exhibits super paramagnetic behaviour. The magnetic properties of CeO_2 doped Fe_2O_3 reduces with increase of cerium oxide concentration. Moreover, the H_c of ceria 10% doped Fe_2O_3 calcined at 600 °C/2 hours nano-particulates and show maximum H_c which might be due to localized effect of Ce^{4+} ion to Ce^{3+} ion occurrence with optimum distortion[28-30].

5 Conclusion

The co-precipitation method was used to synthesize CeO_2-doped Fe_2O_3 nanoparticles, resulting in a reduction of particle size as indicated by XRD analysis, which showed a decrease from 60.547 nm to 47.060 nm. The FTIR analysis revealed characteristic peaks corresponding to hydroxyl group vibrations at 3541 cm^{-1}, 2200 cm^{-1}, and 1624 cm^{-1}, while sharp peaks at 614 cm^{-1} and 471 cm^{-1} were attributed to O-Fe-O and O-Ce-O molecules vibrations, respectively. The VSM tools analysis demonstrated that the saturation magnetisation and remnant magnetisation (M_r) decreased with increasing concentrations of cerium oxide (5%, 10%, and 20%). Consequently, these nanoparticles, characterized by reduced size, altered magnetic properties due to doping and hold potential for diverse applications such as drug delivery, and magnetic storage devices.

References

1 Materón E M, Miyazaki C M , Carr O, Joshi N, Picciani P H S, Dalmaschio C J, Davis F & Shimizu F M, *Appl Surf Sci Adv*, 6 (2021) 100163.
2 Aslani F, Bagheri S & Zulkapli N M, *Growth: An Overview Sci World J*, 641759 (2014); https://doi.org/ 10.1155/ 2014/641759.
3 Benhammada S A, Trache D, Kesraoui M, Tarchoun A F, Chelouche S, Mezroua A, *Thermochimica Acta,* (2020) 178570.
4 Ounacer M, Essoumhi A, Sajieddine M, Razouk A, Costa B F O, Dubiel S M & Sahlaoui M, *J Supercond Novel Magn,* 33 (2020) 3249.
5 Yao R & Cao C, *RSC Adv*, 2 (2012) 1979.
6 Malik V, Sen S, Gelting D R, Josifovska M G, Schmidt M & Guptasarma P, *Mater Res Express*, 1 (2014) 026114.
7 Bouzigues C, Gacoin T & Alexandrou A, *ACS Nano*, 5 (2011) 8488.
8 Peters J A, *Prog Nucl Magn Reson Spectrosc*, 120 (2020) 72.
9 Zhao X, Zhao H, Chen Z & Lan M, *J Nanosci. Nanotechnol*, 14 (2014) 210.

10 Laurent S, Bridot J L & Elst L V, *Future Med Chem,* 2 (2010) 427.

11 Dutz S & Hergt R, *Nanotechnology,* 25 (2014) 452001.

12 Deatsch A E & Evans B A, *J Magn Magn Mater*, 354 (2014) 163.

13 Pankhurst Q A, Connolly J, Jones S K & Dobson, *J Phys D Appl Phys,* 36 (2003) R167.

14 Brero F, Albino M, Antoccia A, Arosio P, Avolio M, Berardinelli F, Bettega D, Calzolari P, Ciocca M & Corti M, *Nanomaterials*, 10 *(*2020) 1919.

15 Dahle J T & Arai Y, *Int J Environ Res Public Healt*, 12 (2015)1253.

16 Ascencio F, Rangel-Gamboa L, Maqueda-Cabrera B, Zorrill C, Herrera R & Mendoza-Cruz R, *Mater Chem Phys,* 311 (2024 128492.

17 Nadjia L, Abdelkader E, Naceur B & Ahmed B , *J Rare Earths,* 36 (2018) 575.

18 Zhao H P, Zhu M L, Shi H-Y, Zhou Q-Q, Chen R, Lin S-W, Tong M-H, Ji M-H, Jiang X, Liao C-X, Chen Y-X & Lu C-Z, *Molecules,* 27 (2022) 9050.

19 To T D, Nguyen H G T, Doan T C D & Shiratori Y, *Int J Nanotechnol,* 15, (2018) 11/12.

20 Kiziltaş H, Tekin T & Tekin D, *J Environ Chemi Eng.* 8 (2020) 104160.

21 Kumar V, Ahlawat D, Islam S A & Singh A, *Mater Sci Eng B*, 272 (2021) 115327.

22 Umamaheswari G T, Surumbarkuzhali N, Kulathooran K, Subramani S, Thangarasu R, Arunachalam S & Kumar M, *Digest J Nanomater Biostruct,* 17 (2022) 1135.

23 Pena-Garcia R, Guerra Y, Farias B V M, Santos F E P, Nobre F X, Caland J P, Pessoni H S V, Franco A, Padron-Hernández E, *Ceram Int,* 45 (2019) 918.

24 Justus J S, Dharma R S D & Ezhil R A M, *J Appl Sci Eng Methodol*, 2 (2016) 272.

25 Kant R, Kumar D & Dutta V, *RSC Adv,* 5 (2015) 52945.

26 Priyadarshini S, Pai B D & Nayak S K, *J Mater Sci,* (2015) **DOI:** 10.1007/s10853-015-8987-8.

27 Saberi A, Golestani-Fard F & Sarpoolaky H, *J Alloys Compd,* 462, (2008) 142.

28 Khan S B, Faisal M, Rahman M M & Jamal M, *Int J Electro Chem Sci,* 8 (2013) 7284e97.

29 Saini J, Sharma M & Kuanr B K, *Nanoscale Adv*, 3 (2021) 6074.

30 Li L, Chu Y & Liu Y, *Nanotechnology,* 18 (2007) 105603.

31 Jacob J & Abdul K M, *J Magn Magn Mater*, 322 (2010) 614.

32 Sharma R, Hooda N, Hooda A & Khasa S, *J Alloys Compd*, 965 (2023) 171394.